Supplemental Material

S1. Watershed and soil attributes

S1.1 Extent of wetlands and lakes

Estimates of lake and wetland cover were extracted from the Province of British Columbia Terrestrial Ecosystem Mapping (TEM) (Green, 2014; Gonzalez Arriola et al., 2015). The estimate of wetland cover is derived by combining the cover of nine ecosystem classes typically considered to have wet (hygric to subhydric) to very wet (hydric) soils, including blanket bogs, bog woodlands, basin bogs, fens and swamps (Banner et al., 1993, MacKenzie and Moran, 2004). This metric omits the widespread bog forests of Calvert and Hecate Islands, which have very moist (subhygric) to wet soil moisture regimes (Banner et al., 1993) and are transitional between upland and wetland ecosystems. The TEM dataset has polygons containing up to three ecosystem classes, with no information on the location of classes within polygons. Where TEM a polygon was intersected by watershed boundaries, we assumed a homogenous distribution of ecosystem classes within the polygon. After summing the cover of wetlands in each watershed we calculated the percentage of land (watershed area less lakes) covered by wetlands.

S1.2 Soil sampling and depth predictions

Soil data were collected at a total of 353 field sites. Of these sites, 322 were located at fixed distances along transects established using a conditioned latin hypercube sampling design (Minasny and McBratney, 2006). The transect method was adopted because access on this remote island is restricted, and it was not possible to visit all of the points identified in the original hypercube procedure. The effect was to have small clusters of points that were well - distributed and representative of the study area. At all sites, the thickness of organic horizons,

thickness of mineral horizons, and total soil depth to bedrock were recorded, along with observations needed for categorization according to the Canadian System of Soil Classification (Soil Classification Working Group, 1998) and the British Columbia terrain classification (Howes and Kenk, 1997). For some sites, total depth exceeded the reach of sampling tools, so recorded thicknesses were likely conservative. Data were also collected at an additional 31 sites that were located in previously established ecosystem inventory plots with the same soil attributes (Giesbrecht et al., 2015). In addition to field-sampled points, 40 sites with exposed bedrock (0cm soil depth) were located using aerial photography.

Total organic horizon thickness, total mineral horizon thickness, and total soil depth were combined with a suite of topographic, vegetation, and remote sensing data for each sampling point, and the resulting dataset was used to train a random forest model (randomForest package in R; Liaw and Wiener, 2002) which predicted soil depth values and soil/terrain types for all points on the landscape. Depth predictions represent a modification of the procedure used by Scarpone et al. (2016) for depth predictions in interior British Columbia.

S2. Hydrology- Rating curve calculations of stream discharge and error analysis

S2.1 Stage Measurements

Stations were installed in the spring and early fall of 2014 as part of a telemetry network allowing for near real time download of data. At each station, an OTT PLS – L (OTT 2016) pressure transducer (0 - 4 m range SDI-12) was installed. Each sensor was connected to a CR1000 (Campbell Scientific, 2015) data logger. Stage measurements were recorded every five minutes with a five second sampling interval and mean, max, min and standard deviation of stream stage recorded over each five minute period. Each watershed also had stand-alone Odyssey Capacitance Water Level recorder (Data Flow Systems PTY Ltd 2016) installed in

proximity to the pressure transducer to act as a back-up in case of sensor or data logger malfunction.

S2.2 Discharge Measurements

Stream discharge was measured using multiple methods. Low and moderate flows, generally below 0.5 $m^3 s^{-1}$, were measured using the velocity area method midsection discharge equation (ISO, 1992; ISO, 1997). The flow velocities were measured with the Swoffer 2100 propeller type mechanical current meter (Swoffer Instruments Inc., Seattle, USA) or the Sontek Flowtracker acoustic doppler velocimeter (SonTek, San Diego, USA). Flow velocities were averaged by the Swoffer over a five second measurement interval and by the Flowtracker over a 30 second measurement interval for each location. A suitable river cross-section site was defined by: a) general flow direction perpendicular to the cross-section line, b) uniform stream bed conditions, and c) constrained flow conditions with no back eddies and low turbulence. At some watersheds, multiple velocity-area sites were used depending on conditions at time of measurement.

At flows greater than 0.5 $m^3 s^{-1}$, salt dilution was the primary method to measure discharge, specifically salt in solution ("salt solution") as described by Moore (2005). Discharge was calculated using the following formula:

$$Q = \frac{V}{\sum RC_t \cdot t_{int}} \quad (4)$$

where V represents the volume of salt solution (m^3), RC_t the relative concentration of salt solution (mL mL^{-1}) and t_{int} is the time interval of measurement. RC_t is obtained using a relative concentration, related to electrical conductivity (EC):

$$RC_t = (EC_t - EC_0) \cdot CF \quad (5)$$

where EC_t is the temperature corrected EC measured at time t ($\mu S\ cm^{-1}$), EC_0 is the baseline conductivity of the stream ($\mu S\ cm^{-1}$) defined as the five minute average prior to the salt wave, and CF is the calibration factor. The end of the salt wave was defined as the point in which the five minute EC average equaled EC_0. In some instances the post-five minute average would not return to EC_0 due to changes in background chemistry not associated with the salt dump. When this occurred, EC_0 was determined by linear interpolation for baseline EC, pre and post measurement.

The CF is defined as the relationship between additions of primary solution (made up of salt solution and stream water) to a known volume of secondary solution (stream water only), with the resulting slope of the line corresponding to the CF value. The primary solution was typically made up of 10 mL salt solution (used in discharge measurement) added to 1000 mL of stream water. Then, 2 or 5 mL increments of the primary solution was pipetted into 3000 mL of the secondary solution, and corresponding changes in EC were recorded. Linear regression was performed to determine slope of the line.

Due to difficulties associated with being on location to measure high discharge, a "salt dilution system" was designed using the salt solution method described above. The system was entirely automated and located within an extensive telemetry network enabling remote activation off-site or through pre-programmed stream stages where discharge measurements had not been previously measured.

A volume of salt solution, stored in two, 200 L barrels on site, allowed for up to thirty measurements between refills. Recharging of the salt solution reservoir was done manually and the CF completed following the refill and prior to the next refill (the reservoir was designed to ensure that at least 5 L of solution remained after the final discharge measurement), for a

92 minimum of two CF's between refills. When the water level reached a predefined stage, a signal
93 was sent to release a pre-determined volume of salt solution from a reservoir connected to the
94 salt solution storage barrels. To increase the accuracy of this volume, the salt solution was first
95 pumped into a stainless steel cylinder with a pressure transducer at the bottom to measure water
96 depth, and in turn volume. The solution was then transferred to a dumping mechanism located
97 above the stream designed for near instantaneous release. Upon initiation of the salt solution
98 dump sequence, a second command was sent to a downstream data logger to activate two Global
99 Water-WQ Cond sensors (Global Water instrumentation, Inc., College Station, USA) to measure
100 EC_t at one second intervals, and therefore capture the passing salt wave. Once the dump
101 sequence was completed, the EC_t data were transmitted via the telemetry network to a server
102 accessed via the internet. The volume of salt depended on estimated discharge measurements,
103 with maximum EC measurements targeted to be no more than 40 uS above background, well
104 below the most sensitive toxicity threshold of 400 mg L^{-1} (Moore 2004a, 2004b).

105 **S2.3 Error and uncertainty analysis**

106 **S2.3.1 Discharge measurement error analysis**

107 Errors associated with manual direct discharge measurements were estimated using
108 statistical techniques and on-site observations. For the velocity-area method, discharge
109 uncertainty was calculated using the Interpolated Variance Estimator (IVE) (Cohn et al., 2013).
110 For the salt dilution method, a statistical and site specific uncertainty estimation method was
111 developed.

112 **S2.3.2 Uncertainty analysis for the velocity-area measurements**
113
114 As described in Cohn et al. (2013), the IVE was used to estimate uncertainty in velocity
115 area discharge measurements. It is based on the assumption that depth and velocity vary

gradually across a channel cross-section and that depth and velocity vary linearly between adjacent stations. The difference between the assumed and the measured value is used to calculate measurement uncertainty. In addition, uncertainties associated with calibration and systemic errors in the width, depth, and velocity were assumed to be 1% for the Sontek Flowtracker (the accuracy of the device calibration; Sontek/YSI, 2007) and 5% for the Swoffer current meter, due to increased potential uncertainty from the shorter time interval used to determine average velocity. Total uncertainty was estimated based on the above uncertainties and the number of measurement stations (see Cohn et al. 2013).

S2.3.3 Salt dilution discharge uncertainty

The discharge uncertainty for salt dilution measurements was estimated using the sensor resolution, calibration errors, salt volume errors, and salt mixing errors. Uncertainty (u_Q), associated with discharge calculated from a conductivity sensor is based on the following:

$$u_Q = u_v + \frac{\sum_{i=1}^{m}((u_{EC,i} + u_{CF})C_i)}{\sum_{i=1}^{m} C_i} \quad (6)$$

Where u_v is the relative uncertainty due to salt volume error (%), $u_{EC,i}$ is the relative uncertainty in EC measurement i due to the resolution of the sensor (%), u_{CF} is the relative uncertainty in CF (%), C_i is the calculated salt concentration at measurement i (g m^{-3}), and m is the total number of EC measurements.

Error associated with determining the volume of salt (u_v) was estimated by:

$$u_v = \frac{\Delta v}{v} \cdot 100 \quad (7)$$

where V is the volume of salt solution released to the stream (L), and ΔV is the estimated error in salt solution volume (L). The error in solution volume was estimated based on the resolution (1 mm) of the pressure transducer inside the stainless steel cylinder salt dump reservoir. With an

uncertainty of 0.5 mm in solution height inside the cylinder and a cylinder diameter of 304 mm, the uncertainty in solution volume for each release was 36.3 mL. Because the cylinder was never completely emptied, two level measurements were made to calculate water, thus total maximum error in solution volume (ΔV) was 72.6 mL.

Electrical conductivity measurement uncertainty (u_{EC}), dependent on the resolution of the conductivity sensor (Res) is described below:

$$u_{EC} = \frac{0.5 \cdot Res}{EC} \cdot 100 \quad (8)$$

Uncertainty related to u_{CF} was a function of the errors associated with the measurement of salt concentration of the primary and secondary solution, a combination of volumetric error of the primary solution (±0.3 mm, volumetric flask precision), the secondary solution (±3.0 mm volumetric flask precision plus rain splash and field conditions) and each primary solution dose (0.006 mL, based on precision of the pipette) added in 2 or 5 mL increments. Uncertainty of the CF was derived from the maximum variation in slope, a product of the salt concentration error ranges. The calibration regression curve was plotted using three data points for each conductivity measurement: the assumed salt concentration, the assumed salt concentration plus maximum error, and the assumed salt concentration minus maximum error (Figure S2.1). Next, the maximum variation of slope was calculated using the standard deviation of slope (σ_s):

$$\sigma_s = \sqrt{\frac{(\frac{1}{n-2}) \sum_{i=1}^{n} (y_i - \hat{y}_i)^2}{\sum_{i=1}^{n} (x_i - \bar{x})^2}} \quad (9)$$

where n is the number of data points, y_i is the assumed salt concentration (± error) of measurement i (mL mL^{-1}), $\hat{y}_i$ is the modelled salt concentration (mL mL^{-1}), x_i is the measured electrical conductivity of measurement i (µS cm^{-1}), and $\bar{x}$ is the mean average electrical

conductivity (μS cm^{-1}). Finally, the CF relative uncertainty (u_{CF}) was defined as two times the standard deviation of slope divided by the CF:

$$u_{CF} = (2 \cdot \sigma_s)/CF \quad (10)$$

If the EC sensors showed different EC readings and confirmed the salt was not completely mixed at the measurement site, additional uncertainty was added to the discharge measurement. To measure the degree of salt mixing at the measurement site, discharges calculated from both conductivity sensor measurements were compared, while taking their uncertainties into account:

$$M = \frac{(Q2-\varepsilon_{Q2})-(Q1+\varepsilon_{Q1})}{(Q1+\varepsilon_{Q1})} \cdot 100 \quad (11)$$

where M is the relative uncertainty due to improper mixing (%), Q1 is the lower discharge value (m^3 s^{-1}), Q2 is the higher discharge value (m^3 s^{-1}), ε_{Q1} is the absolute uncertainty of the lower discharge value, derived from u_Q (Equation 6) and ε_{Q2} is the absolute uncertainty of the higher discharge value. If $M \leq 0$, the salt was assumed to be properly mixed. Any positive outcome of M implies incomplete mixing and is added to the total uncertainty of the discharge measurement.

S2.4 Rating curve development and uncertainty

Discharge is related to stage through the formula:

$$Q = a(h - h_0)^b \quad (12)$$

where Q is discharge (m^3 s^{-1}), h is stage level (m), h_0 is the water level at zero flow (m) and a and b are coefficients specific to the gauging station of a river. The values for h_0, a, and b are obtained by the curve fitting results of simultaneous stage and discharge measurements. For this work, stage-discharge curves were created using a non-linear least-squares fitting Python model (lmfit; LMFit Development Team, 2015). This model approximates the variables (a, b, and h_0) by minimizing the residuals scaled by data uncertainties:

$$[Q_i^{meas} - Q_i^{model}(v)]/\varepsilon_i \quad (13)$$

where Q_i^{meas} is the measured discharge ($m^3\ s^{-1}$), Q_i^{model} is the fitted discharge ($m^3\ s^{-1}$), v the set of variables in the model (a, b and h_0) to be optimized, and ε_i the uncertainty in the discharge measurement. This was a two step process where the curve was first fit taking into account uncertainties related to Q and then fit again taking into account uncertainties in h.

As described above, uncertainty for individual discharge measurements were accounted for in the curve fitting process, with measurements of greater uncertainty having less influence on position of the curve. To account for uncertainty in the stage discharge relation, 95% confidence intervals were created per Herschy (1994) and applied to the final discharge times-series as an estimate of discharge.

S2.5 Results of stream discharge measurement and calculations

A total of 168 total measurements, including 92 measures made using the automated system, were used to develop rating curves for each watershed (Figure S2.1; Floyd et al., 2016). Watershed 703 had the highest total discharge over the study period, which was more than the combined total from watersheds 626, 819, 844 and 1015. Total discharge calculated from the 95% confidence intervals from the rating curves were ±6.5% of the mean of all watersheds, with a range between ±2.93% (708) and ±9.98% (819) (Table S2.3). In general, discharge data from watershed 708 had the lowest uncertainty, due to it having the most discharge measurements and the best developed rating curve. Watershed 819 had the highest uncertainty largely due to the limited number of high flow discharge measurements on the rating curve (max measured was 4.5 m^3s^{-1}) and variation in stage during the discharge measurements at high flow. Four of the seven watersheds had total discharge measurements less than ±5.0% of the estimated measurements

from the rating curve, and none were > 10% for the entire project study period, however for water year 2015/2016, 819 had a total discharge uncertainty of ±13.0%.

Figure S2.1. Stage discharge rating curves for seven focal watersheds. Confidence intervals (95%) are calculated based on Herschy (1994). Error bars represent uncertainty from individual measurements.

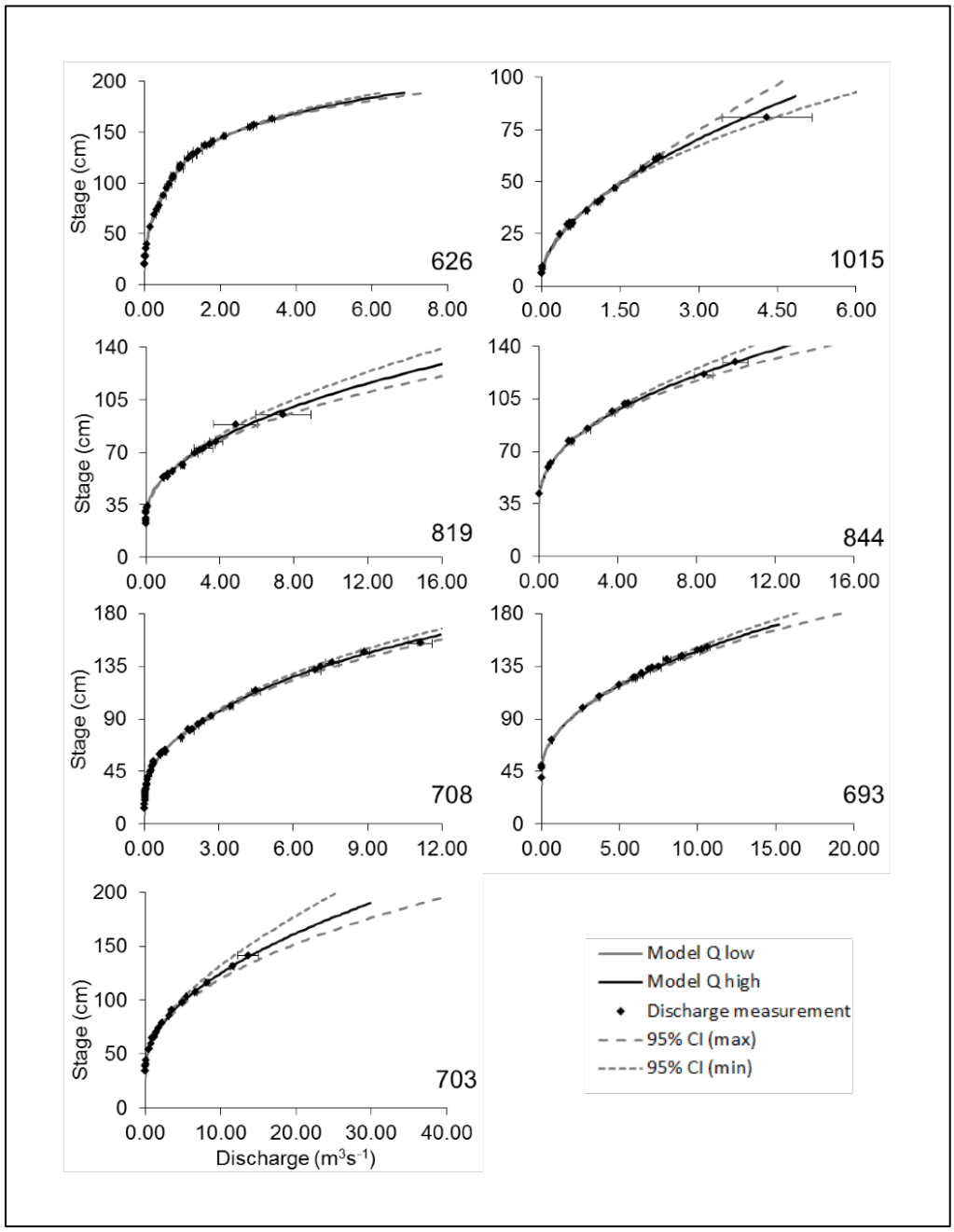

Table S2.3. Uncertainty (%) in total discharge, by water year and over the entire study period, based on rating curve confidence intervals (95%). Values are plus or minus the modelled output**.**

Watershed	*2014-15*	*2015-16*	*2014-2016*
626	5.57	5.54	5.55
693	3.35	2.97	3.19
703	10.14	9.37	9.83
708	2.93	2.93	2.93
819	7.49	13.01	9.98
844	4.98	4.47	4.78
1015	9.01	8.58	8.84

S3. Generating model estimates of DOC flux using rloadest

Table S3.1: The number of samples and specific regression model used by rloadest for calculating stream loads. Estimated bias of each model shows relatively low overall bias for each model, with 844 clearly showing the highest bias.

Watershed	n	Model #	Regression model	Estimated % bias
626	23	7	$a_0 + a_1 \ln Q + a_2 \sin(2\pi dtime) + a_3 \cos(2\pi dtime) + a_4\, dtime$	2.026
1015	24	7	$a_0 + a_1 \ln Q + a_2 \sin(2\pi dtime) + a_3 \cos(2\pi dtime) + a_4\, dtime$	-2.502
819	23	7	$a_0 + a_1 \ln Q + a_2 \sin(2\pi dtime) + a_3 \cos(2\pi dtime) + a_4\, dtime$	2.011
844	20	3	$a_0 + a_1 \ln Q + a_2 dtime$	-11.49
708	24	6	$a_0 + a_1 \ln Q + a_2 \ln Q^2 + a_3 \sin(2\pi dtime) + a_4 \cos(2\pi dtime)$	-0.206
693	23	6	$a_0 + a_1 \ln Q + a_2 \ln Q^2 + a_3 \sin(2\pi dtime) + a_4 \cos(2\pi dtime)$	0.092

S4. PARAFAC Modeling of DOM composition

Figure S4.2: Fingerprint map showing the six fluorescence components determined by PARAFAC analysis.

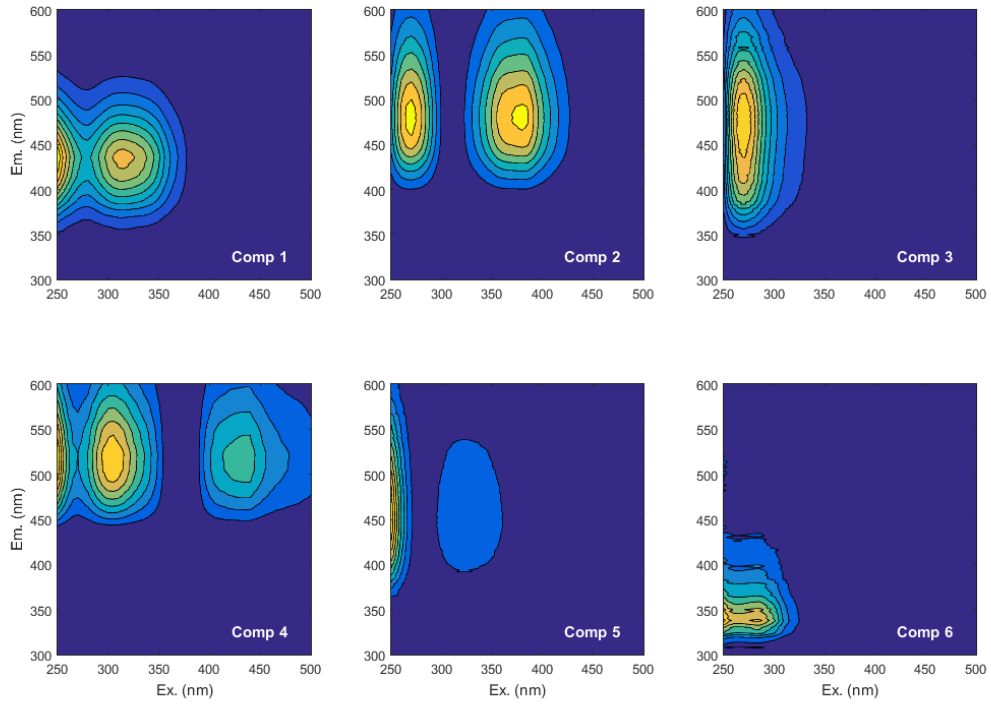

Figure S4.3: Split half validation plots for the six fluorescence components determined by PARAFAC analysis.

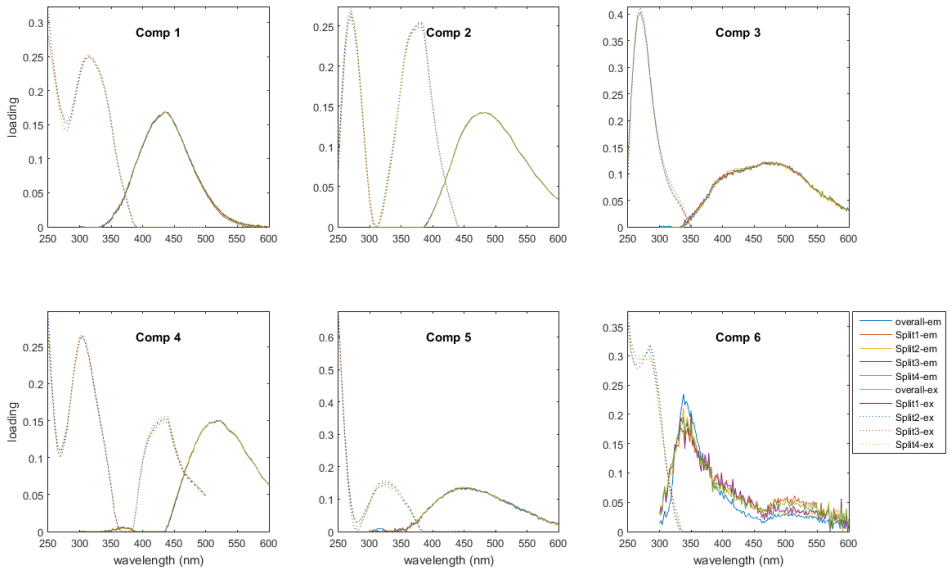

Figure S4.4: Box plots showing the percent contribution to total fluorescence from each of the six components determined by PARAFAC analysis for each of the seven watersheds used in this study.

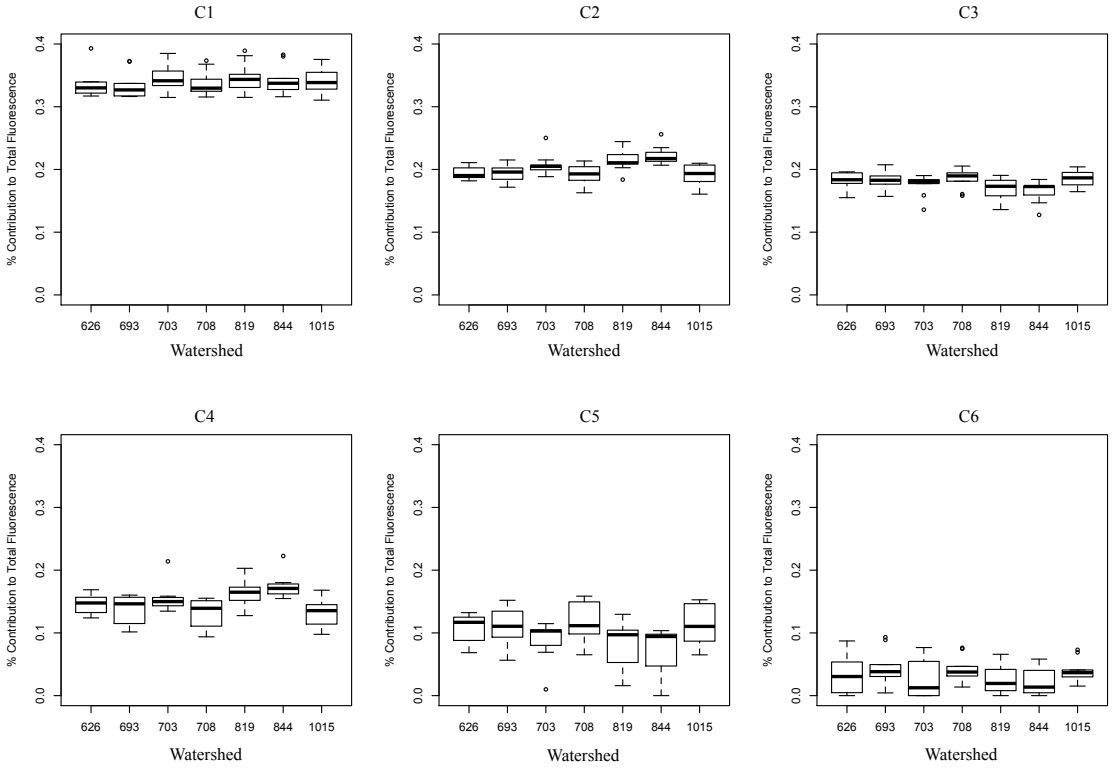

Table S4.1: Locations of maximum fluorescence values and the corresponding excitation and emission wavelengths for each of the six peaks (components) determined with PARAFAC modelling.

Component	Excitation (nm)	Excitation F_{max}	Emission (nm)	Emission F_{max}
1	315	0.2502	436	0.1688
2	270	0.2607	484	0.1422
	380	0.2539		
3	270	0.4125	478	0.1212
4	305	0.2648	522	0.1504
	435	0.1512		
5	325	0.1408	442	0.1321
6	285	0.3108	338	0.2350

S5. Redundancy analysis: Relationships between watershed characteristics and DOC exports

Figure S5.1: Partial-RDA Axis 1 versus Axis 3. RDA was performed under type 2 scaling.

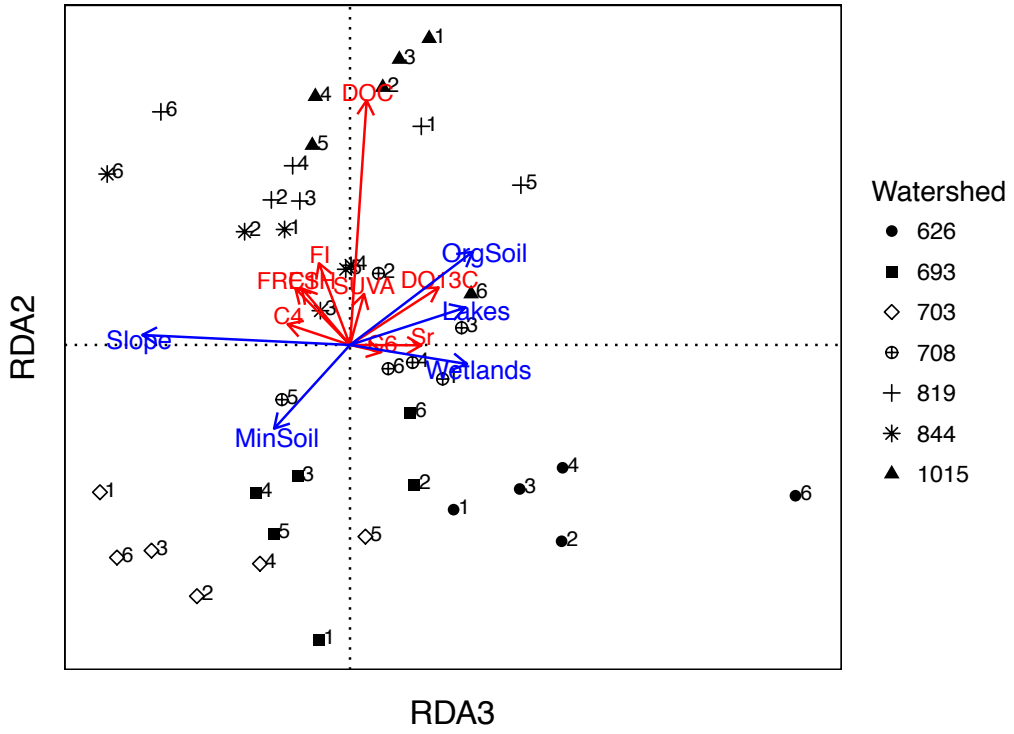

Figure S5.2: Partial-RDA Axis 2 versus Axis 3. RDA was performed under type 2 scaling.

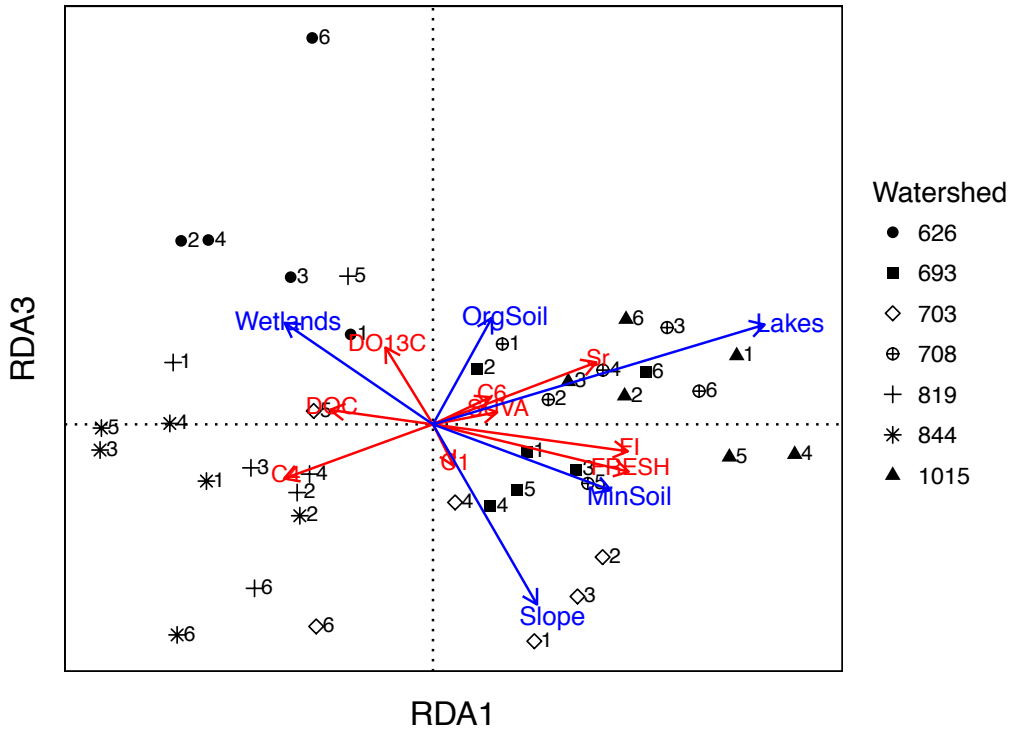

Table S5.3: Relative eigenvalues and the statistical significance of each axes in the partial-RDA.

Axis	Eigen -value	F marginal	F forward	P- marginal	P- forward	% total variance in Y	% total variance explained by all axis
1	1.420	18.717	11.047	0.0001	0.0001	15.78	47.3
2	0.902	11.887	9.158	0.0001	0.0001	10.02	30.1
3	0.654	8.622	8.531	0.0002	0.0002	7.27	21.8
4	0.013	0.175	0.175	1.0000	1.0000	0.15	0.4
5	0.011	0.143	0.143	0.9965	0.9965	0.12	0.4

Table S5.4: Results of permutation test on the marginal effects of terms given under the reduced RDA model.

	df	Variance	F	Pr (>F)
Lakes	1	1.093	6.4789	0.001
Slope	1	0.5722	3.392	0.005
Wetlands	1	0.1207	0.7153	0.651
MinSoil	1	0.8403	4.9807	0.001
OrgSoil	1	0.6937	4.1118	0.001
Residual	34	5.7359		

Table S5.5: Biplot scores for partial-RDA axes using type 2 scaling.

	Axis1	Axis2	Axis3	Axis4	Axis5
Lakes	0.8471	0.1028	0.4853	-0.1871	0.0349
Slope	0.2658	0.0275	-0.8769	-0.0410	0.3825
Wetlands	-0.3789	-0.0527	0.4940	0.4033	-0.6664
MinSoil	0.4540	-0.2311	-0.3205	0.1128	0.7905
OrgSoil	0.1503	0.2569	0.5178	0.3138	0.7341

References

Banner, A., MacKenzie, W., Haeussler, S., Thomson, S., Pojar, J., Trowbridge, R.: A field guide to site identification and interpretation for the Prince Rupert forest region, Handbook 26, Res. Br., British Columbia Ministry Forests, Victoria, British Columbia, 42 pp., 1993.

Cohn, T.A., Kiang, J.E., Mason, Jr., R.R.: Estimating Discharge Measurement Uncertainty Using the Interpolated Variance Estimator, American Society of Civil Engineers, doi:10.1061/(ASCE)HY.1943-7900.0000695, 2013.

Floyd, W.C., Korver, M.C., Owen, C., McPhail, J., Brunsting, R., van Meerveld, I.: Stage-discharge time series- Calvert Island, Hakai Institute, doi:dx.doi.org/10.21966/1.243102, 2016.

Giesbrecht, I., Banner, A., Hoffman, K., Sanborn, P., Saunders, S., MacKinnon A.: Ecosystem comparison plots- Calvert Island, Hakai Institute, doi:dx.doi.org/10.21966/1.56481, 2016.

Gonzalez Arriola S., Frazer, G.W., Giesbrecht, I.: LiDAR-derived watersheds and their metrics for Calvert Island, Hakai Institute, doi:dx.doi.org/10.21966/1.15311, 2015.

Green, R.N.: Reconnaissance level terrestrial ecosystem mapping of priority landscape units of the coast EBM planning area: Phase 3, Prepared for British Columbia Ministry Forests, Lands and Natural Resource Ops., Blackwell and Associates, Vancouver, Canada, 2014.

Herschy, R.: The analysis of uncertainties in the stage-discharge relation, Flow Meas. Instrum., 5, 188-190, 1994.

Howes, D.E., and Kenk, E.: Terrain classification system for British Columbia, MOE Manual 10, 2, Province of British Columbia Ministry Environment and Ministry of Crown Lands, Victoria, Canada, 102 pp., 1997.

ISO: Liquid flow measurement in open channels - velocity-area methods, Technical Report 772, International Organization for Standardization, Geneva, Switzerland, available at: www.iso.org, 1979.

ISO Standard 9196: Liquid flow measurement in open channels - Flow measurements under ice conditions, International Organization for Standardization, Geneva, Switzerland, available at: www.iso.org, 1992.

ISO Standard 748: Hydrometry - Measurement of liquid flow in open channels using current-meters or floats, International Organization for Standardization, www.iso.org, 2007.

LMFit Development Team: Lmfit, Least-squares Minimization with Bounds and Constraints, version 0.8.3, available at: http://lmfit.github.io/lmfit-py/, 2015.

MacKenzie, W.H., Moran, J.R.: Wetlands of British Columbia: a guide to identification, Land Manage. Handb. No. 52., Res. Br., British Columbia Ministry Forests, 287 pp., 2004.

Minasny, B., and McBratney, A.B.: A conditioned Latin hypercube method for sampling in the presence of ancillary information, Comput. Geosci., 32, 1378-1388, 2006.

Moore, R.D.: Introduction to salt dilution gauging for streamflow measurement Part I, Streamline Watershed Management Bulletin, 7, 20-23, 2004a.

Moore, R.D.: Introduction to salt dilution gauging for streamflow measurement Part II, constant-rate injection, Streamline Watershed Management Bulletin, 8, 11-15, 2004b.

Moore, R.D.: Introduction to salt dilution gauging for streamflow measurement Part III, slug injection using salt in solution, Streamline Watershed Management Bulletin 8, 1-6. 2005.

Scarpone, C., Schmidt, M.G., Bulmer, C., and Knudby, A.: Modelling soil thickness in the critical zone for Southern British Columbia, Geoderma, 282:59-69, 2016.

Soil Classification Working Group: The Canadian system of soil classification, 3, Publication 1646, Agriculture and Agri-Food, Canada, 187 pp., 1997.

Sontek/YSI: Flowtracker Handheld ADV Technical Manual, Firmware Version 3.3, Software Version 2.20, 2007.